# ALFVÉNIC ELECTRON ACCELERATION IN AURORA OCCURS IN GLOBAL ALFVÉN RESONOSPHERE REGION

PEKKA JANHUNEN[1,5,*], ANNIKA OLSSON[2,†], CHRISTOPHER T. RUSSELL[3] and HARRI LAAKSO[4]

[1]*Department of Physical Sciences, University of Helsinki, P.O. Box 64, FIN 00014, Finland*
[2]*Uppsala Municipality, Office for Children, Youth and Job Market, SE 75375, Uppsala, Sweden*
[3]*Institute of Geophysics and Planetary Physics, University of California, Los Angeles, CA 90024 1567, U.S.A*
[4]*ESA/ESTEC, Code SCI-SH, Noordwijk 2200 AG, The Netherlands*
[5]*Finnish Meteorological Institute, Space Research, P.O. Box 503, FIN 00101, Helsinki, Finland*
[†]*Formerly at Swedish Institute of Space Physics, S-75121 Uppsala, Sweden*
*(*Author for correspondence: E-mail: pekka.janhunen@fmi.fi)*

(Received 24 October 2005; Accepted in final form 30 January 2006)

**Abstract.** Auroral emission caused by electron precipitation (Hardy *et al*., 1987, *J. Geophys. Res.* **92**, 12275–12294) is powered by magnetospheric driving processes. It is not yet fully understood how the energy transfer mechanisms are responsible for the electron precipitation. It has been proposed (Hasegawa, 1976, *J. Geophys. Res.* **81**, 5083–5090) that Alfvén waves coming from the magnetosphere play some role in powering the aurora (Wygant *et al*., 2000, *J. Geophys. Res.* **105**, 18675–18692, Keiling *et al*., 2003, *Science* **299**, 383–386). Alfvén-wave-induced electron acceleration is shown to be confined in a rather narrow radial distance range of 4–5 $R_E$ (Earth radii) and its importance, relative to other electron acceleration mechanisms, depends strongly on the magnetic disturbance level so that it represents 10% of all electron precipitation power during quiet conditions and increased to 40% during disturbed conditions. Our observations suggest that an electron Landau resonance mechanism operating in the "Alfvén resonosphere" is responsible for the energy transfer.

**Keywords:** auroral acceleration, Alfvén waves, Landau resonance

## 1. Introduction

Even as the auroral phenomenon has been studied by many scientists for more than 100 years, we still lack a full understanding of the energisation mechanisms of the aurorae. Magnetospheric processes, driven by the solar wind, force the ionosphere via Joule heating, (mainly), electron precipitation and waves. They all heat the ionosphere, but it is mainly the electron precipitation which is responsible for most of the visible aurora. The average power of electron precipitation is known statistically under different *Kp* conditions. Electron precipitation appears in two main classes, diffuse and discrete, causing diffuse and discrete auroral emission, respectively. The discrete electron precipitation is thought to be mainly energised in the auroral acceleration region at 2–3 $R_E$ (Earth radii) radial distance. The acceleration region separates dense and cold ionospheric plasma from hot and

Space Science Reviews (2006) 122: 89–95
DOI: 10.1007/s11214-006-7017-5

tenuous magnetospheric plasma and is a locus of an upward directed parallel-electric field that accelerates magnetospheric electrons downward.

The idea that Alfvén waves launched from the magnetosphere could accelerate auroral electrons was conceived nearly 30 years ago (Hasegawa, 1976). Later, it was pointed out that at least in some sub-storm-related events, the downward electromagnetic energy flux (Poynting vector) observed at 4–6 $R_E$ is enough to power the intense aurora below (Wygant *et al.*, 2000) and that accelerated electron distributions are seen together with the Alfven waves (Wygant *et al.*, 2002). It was subsequently shown that statistically, the high-altitude downward Poynting vector ($\mathbf{E} \times \mathbf{B}$, where $\mathbf{E}$ and $\mathbf{B}$ are the electric and magnetic fields) carried by Alfvén waves is responsible for 30–35% of the electron precipitation power (Keiling *et al.*, 2003). The altitude where the observed Poynting vector is transferred to electron energisation is according to these studies below the lower range of their measurement radial distance (4–5 $R_E$). Although the question was not explicitly addressed, a common implicit assumption is that the conversion takes place at the auroral acceleration region altitude, i.e. in the same region where significant parallel-electric fields occur.

A statistical study of the plasma density in the auroral region revealed a peculiar island of lower plasma density at 4–5 $R_E$ (Janhunen *et al.*, 2002) radial distance. This island exists only during disturbed geomagnetic activity conditions ($Kp > 2$) and then only in the midnight and evening sectors, i.e. in the same sectors where sub-storm activity is the most common. An island of enhanced electric fields was later found in the electric field statistics, at the same place and with largely similar statistical properties (Janhunen *et al.*, 2004a). Based upon the density observations (Janhunen *et al.*, 2002) one can see that the 4–5 $R_E$ radial distance corresponds approximately to the altitude where the local Alfvén speed is equal to the electron thermal speed, thus allowing Alfvén waves and electrons to become coupled. The magnetic local time (MLT) and *Kp* occurrence pattern of the island is reminiscent of the occurrence pattern of sub-storms. Since sub-storms are generally thought to have an intense Alfvénic wave activity associated with them, by combining these findings and ideas it was suggested that sub-storm-related transient Alfvén waves dump some of their energy to electrons at this altitude, which causes an emptying of the region and (perhaps as a secondary phenomenon depending on non-linear effects) statistically also an enhancement of the electric fields (Janhunen *et al.*, 2004b). This global region was named the Alfvén Resonosphere (ARS).

## 2. Observational Results

Here we take a more direct approach into studying the energy conversion from Alfvén waves to electrons. Using methods similar to Keiling *et al.* (2000) and 5 years of Polar data (1996–2001), so that the full range of altitudes between 5,000 and 30,000 km is now covered, we build a statistical altitude profile of the downward

Poynting vector. The dataset is also such that if taken as a three-dimensional dataset consisting of ($R$, MLT, ILAT) bins, all bins have significant orbital coverage for both low and high $Kp$, i.e. the dataset is practically free of orbit aliasing effects. Conversion of electromagnetic energy to electron energy is seen as a non-zero divergence (sink) of the Poynting vector, i.e. a radial positive derivative of the downward Poynting vector component. The data used from Polar are the electric and magnetic field instruments EFI (Harvey *et al.*, 1995) and MFE (Russell *et al.*, 1995). To exclude the DC Poynting vector we subtract a low-pass filtered version of the measured magnetic field. We tested two types of filters, one which is fixed in frequency (Keiling *et al.*, 2003) and another one whose cutoff frequency varies with altitude so as to give a constant spatial wavenumber cutoff (measured at the ionospheric plane). The results of these two approaches are qualitatively similar and thus, here we only report the results using the spatial filters.

Figure 1 presents the statistics of the downward Poynting vector against the radial distance from the Earth's centre using all measurements collected in the nominal auroral zone, that is, in the 18–06 MLT sector and at 65–74° invariant latitude (ILAT). One can distinguish a clear stepwise transition in amplitude of the downward Poynting vector at 4–4.5 $R_E$, particularly during high $Kp$. This is exactly the same altitude where the island of low plasma density and higher electric fields are detected (Janhunen *et al.*, 2002, 2004a,b). For $Kp \leq 2$ almost no stepwise transition occurs, for $2 < Kp \leq 4$ the transition is clear and for $Kp > 4$ it is strong. Varying the spatial filter cutoff between 20 and 200 km causes a variation in the amplitude of the step, but does not change the conclusion that the main energy deposition occurs at 4–5 $R_E$.

In the next step, we characterise the change of the Poynting vector in more detail. Figure 2 shows the radial derivative of the downward Poynting vector component and plots the results against radial distance and ionospheric scale. The scale is the mapped-down perpendicular scale size which has been inferred from the time-domain satellite data under the assumption of static structures through which the satellite moves at its known orbital velocity. Here the analysis is run for four spatial band-pass filters, while in Figure 1 we used spatial low-pass filters. One can see that for $Kp \leq 2$ no identifiable structured energy deposition occurs, but for $2 < Kp \leq 4$, enhanced deposition occurs at 4–5 $R_E$ at all scales, especially scales 50–100 km are preferred (the scale here is related to the latitudinal width of the electron precipitation region in the ionosphere). For $Kp > 4$ the same structured deposition occurs, but the most intense deposition now takes place at smaller scales (20–50 km). One needs to notice that the higher the $Kp$ value, the smaller the number of events and the larger the statistical scatter, and thus, all features in the $Kp > 4$ map may not be statistically significant. Nevertheless, the firm conclusion is that the main energy deposition occurs in the ARS region (4–5 $R_E$ radial distance).

We continue the analysis by averaging the downward Poynting vector below 3.5 $R_E$ and above 4.5 $R_E$, and calculating their difference that yields the total power deposited in the ARS region. The purple bars in Figure 3 show the results for the

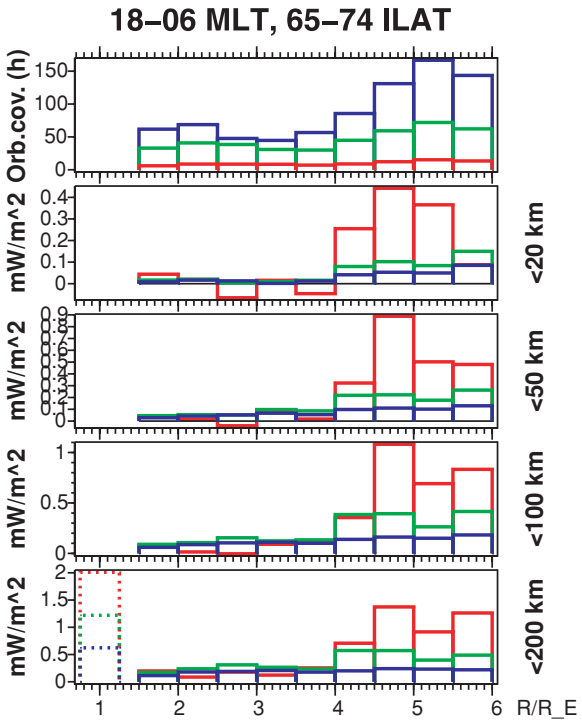


*Figure 1.* Downward parallel-Poynting vector plotted against geocentric (radial) distance $R$ in the nightside auroral zone [18–06 magnetic local time (MLT), 65–74 invariant latitude (ILAT)]. Because the amplitudes of wave electric and magnetic fields increase with decreasing distance to the Earth due to the converging geomagnetic field, the amplitudes of the Poynting vectors have been mapped accordingly to the ionospheric plane, assuming wave energy conservation in the flux tube. Top panel is orbital coverage in hours for each bin. Other panels are the downward component of the Poynting vector in milliwatt per square meter computed with magnetic field that has been spatially low-pass filtered so that only the ionospheric scales given on the right-hand side are retained (assuming that the satellite but not the structure is moving). Key: $Kp \leq 2$ is *blue*, $2 < Kp \leq 4$ is *green*, $Kp > 4$ is *red*, where the first range is for low magnetic activity in space, the second is for moderate activity, and the third is for high activity. Bottom panel shows also the electron precipitation power from Hardy's statistical model1 by *dotted lines*.

three *Kp* ranges; the blue bars give the statistically known amount of total auroral electron precipitation (Hardy *et al.*, 1987). This reveals that the fraction of the ARS-related Alfvénic electron precipitation increases steeply with the *Kp* index.

## 3. Discussion and Conclusions

The observational evidence is convincing that the ARS region forms where the local Alfvén speed coincides with the local electron thermal speed, bringing the Alfvén

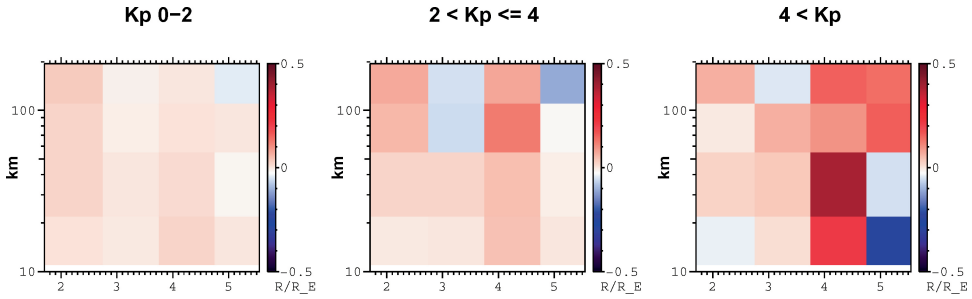


*Figure 2.* Distribution of radial derivative of downward Poynting vector component as a function of radial distance (horizontal axis) and ionospheric scale size (vertical axis). In each bin the quantity shown has units mW/m$^2$/$R_E$, and tells how much power is transferred from waves to electrons per Earth radius. *Blue colour* suggests that the energy is transferred from electrons to waves, but it should be seen as statistical noise. One can see the critical region to appear at 4–5 $R_E$ and the preferred scales for waves are 50–100 km for moderate *Kp* and 20–50 km for high *Kp*.

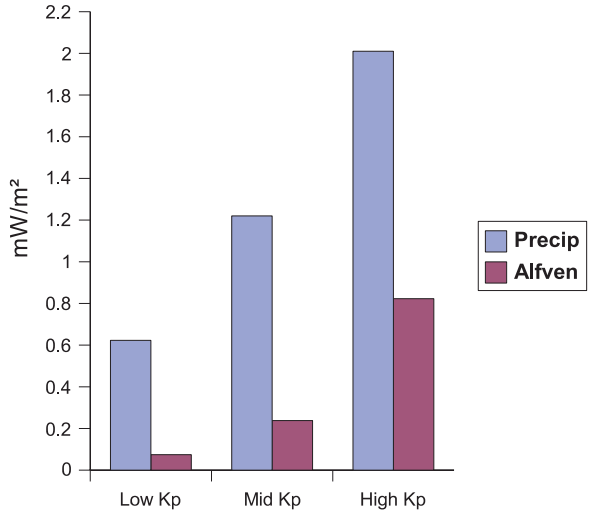


*Figure 3.* Power density of electron precipitation [after Hardy's statistical model (Hardy *et al.*, 1987)] and the decrease of the power density of the Poynting vector in the Alfvén Resonosphere. The three *Kp* ranges are $Kp \leq 2$ (low), $2 < Kp \leq 4$ (mid), $Kp > 4$ (high). The Alfvénic vs. total electron precipitation fractions are 10, 20 and 40%, respectively for low, mid and high *Kp* ranges.

waves into Landau resonance with some of the electrons (Figure 4). In the process the Alfvén waves probably undergo spectral redistribution to smaller scales where the wave character becomes kinetic and enables coupling to electrons (Voitenko and Goossens, 2005). Some indications of this spectral shift can be seen in Figure 1. While this picture is simple and understandable, in reality, kinetic, non-local and non-linear effects (Lysak and Lotko, 1996) can modify the place where the most efficient energy conversion occurs. Most of these complications are included in

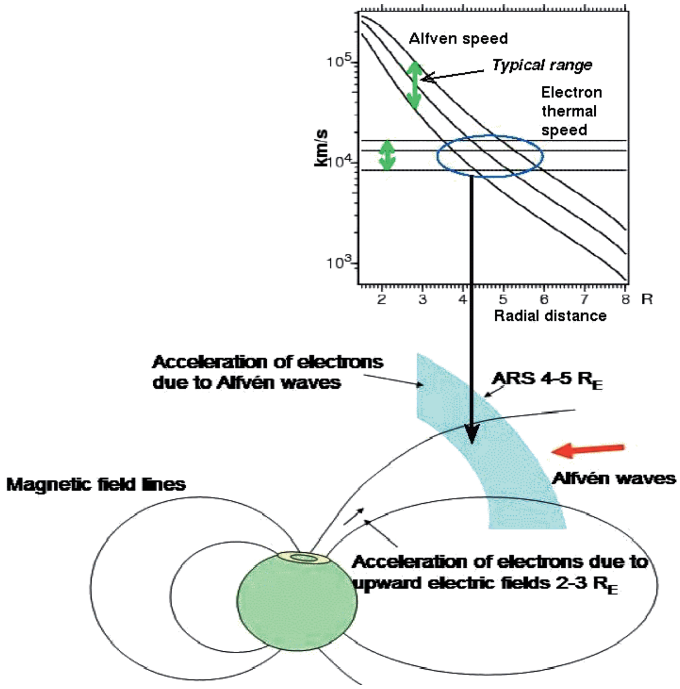


*Figure 4.* Schematic location of Alfvén resonosphere in near-Earth space at 4–5 $R_E$ radial distance. The normal auroral acceleration region at 2–3 $R_E$ is also shown. The diagram shows the typical range of the Alfvén wave speed and electron thermal speeds against radial distance. Notice that even in the presence of some uncertainty in the numerical values of both speeds, the radial range where these speeds are equal is rather narrow and well defined, thanks to the cubic dependence of the geomagnetic field and Alfvén speed on $1/R$.

recent theoretical models (Lysak and Song, 2003). The results of these models depend on a number of parameters and assumptions, but they generally predict that the most efficient conversion takes place at a somewhat lower altitude than 4–5 $R_E$ (Lysak and Song, 2003). Thus, more work remains to be done to bring the theory and observations to quantitative agreement.

Our results indicate that auroral electron energisation and precipitation cannot be explained by one mechanism but they are a superposition of two processes that differ by location and dynamics: electrostatic acceleration in the acceleration region at 2–3 $R_E$ and Alfvénic acceleration at 4–5 $R_E$ . The Alfvénic acceleration is energetically important only during disturbed conditions and it is probably responsible for the field-aligned electrons observed by low orbiting satellites mainly in the plasma-sheet boundary layer (Chaston *et al.*, 2002). The microphysical details of both acceleration mechanisms are still unclear, but understanding them should be more tractable now that their spatial limits and dynamical behaviour are known statistically.

The global ARS region has an impact on all studies of the auroral magnetosphere, in addition to its role in global dynamics and energy conversion processes. The ARS concept should also be applicable to the aurora of other magnetised planets.

## Acknowledgement

We are indebted to the Polar team for the high-quality data they produce for the community.

## References

Chaston, C. C., Bonnell, J. W., Peticolas, L. M., Carlson, C. W., McFadden, J. P., and Ergun, R. E.: 2002, *Geophys. Res. Lett.* **29**(11), p. 30, CiteID 1535.

Hardy, A., Gussenhoven, M. S., Raistrick, R., and McNeil, W. J.: 1987, *J. Geophys. Res.* **92**, 12275.

Harvey, P., Mozer, F. S., Pankow, D., Wygant, J., Maynard, N. C., and Singer, H.: 1995, *Space Sci. Rev.* **71**, 583.

Hasegawa, A.: 1976, *J. Geophys. Res.* **81**, 5083.

Janhunen, P., Olsson, A., and Laakso, H.: 2002, *Ann. Geophys.* **20**, 1743.

Janhunen, P., Olsson, A., and Laakso, H.: 2004a, *Ann. Geophys.* **22**, 1233.

Janhunen, P., Olsson, A., Hanasz, J., Russell, C. T., Laakso, H., and Samson, J. C.: 2004b, *Ann. Geophy.* **22**, 2213.

Keiling, A., Wygant, J. R., Cattell, C. A., Mozer, F. S., and Russell, C. T.: 2003, *Science* **299**, 383.

Lysak, R. L. and Lotko, W.: 1996, *J. Geophys. Res.* **101**, 5085.

Lysak, R. L. and Song, Y.: 2003, *J. Geophys. Res.* **108**(A8), SMP 9-1, CiteID 1327.

Russell, C. T., Snare, R. C., Means, J. D., Pierce, D., Dearborn, D., and Larson, M.: 1995, *Space Sci. Rev.* **71**, 563.

Voitenko, Y. and Goossens, M.: 2005, *Phys. Rev. Lett.* **94**(13), 135003.

Wygant, J. R., Keiling, A., Cattell, C. A., Johnson, M., Lysak, R. L., Temerin, M., Mozer, F. S., Kletzing, C. A., Scudder, J. D., Peterson, W., Russel, C. T., Parks, G., Brittnacher, M., Germany, G., and Spann, J.: 2000, *J. Geophys. Res.* **105**, 18675.

Wygant, J. R., Keiling, A., Cattell, C. A., Lysak, R. L., Temerin, M., and Mozer, F. S.: 2002, *J. Geophys. Res.* SMP 42-1, CiteID 1201, doi 10.1029/2001JA900113.